High-precision computations of divergent asymptotic series and homoclinic phenomena

Vassili Gelfreich*
Carles Simó**

* Mathematics Institute, University of Warwick,
Coventry CV4 7AL, United Kingdom
E-mail: gelf@maths.warwick.ac.uk

** Departament de Matemàtica Aplicada i Anàlisi, Universitat de Barcelona,
Gran Via 585, 08007 Barcelona (Spain)
E-mail: carles@maia.ub.es

November 21, 2006

Abstract

We study asymptotic expansions for the exponentially small splitting of separatrices of area preserving maps combining analytical and numerical points of view. Using analytic information, we conjecture the basis of functions of an asymptotic expansion and then extract actual values of the coefficients of the asymptotic series numerically. The computations are performed with high-precision arithmetic, which involves up to several thousands of decimal digits. This approach allows us to obtain information which is usually considered to be out of reach of numerical methods. In particular, we use our results to test that the asymptotic series are Gevrey-1 and to study positions and types of singularities of their Borel transform. Our examples are based on generalisations of the standard and Hénon maps.

1 Introduction

One of the most popular examples which exhibits exponentially small splitting of separatrices is the standard map defined by $(x, y) \mapsto (x_1, y_1)$, where

$$y_1 = y + \varepsilon \sin(x), \qquad x_1 = x + y_1, \tag{1}$$

and ε is a small positive parameter. This map is used as a model in various branches of Mathematics and Physics. The origin is a hyperbolic fixed point of the standard map, and its separatrices look similar to a separatrix of the mathematical pendulum defined by the differential equation

$$\ddot{x} = \sin x.$$

The stable and unstable separatrices of the pendulum coincide. On the other hand, the stable and unstable separatrices of the standard map cannot coincide due to analytical obstacles. We say that the invariant manifolds of the map are split. They have a primary intersection at a point with $x = \pi$ due to a symmetry (see Fig. 1). Transversality of separatrices at a homoclinic point has important consequences for the dynamics. Usually the splitting of invariant manifolds is studied using the Melnikov method [8, 1, 2]. In the case of the standard map and most of its generalisation the Melnikov methods fails [6]. Lazutkin [7] derived

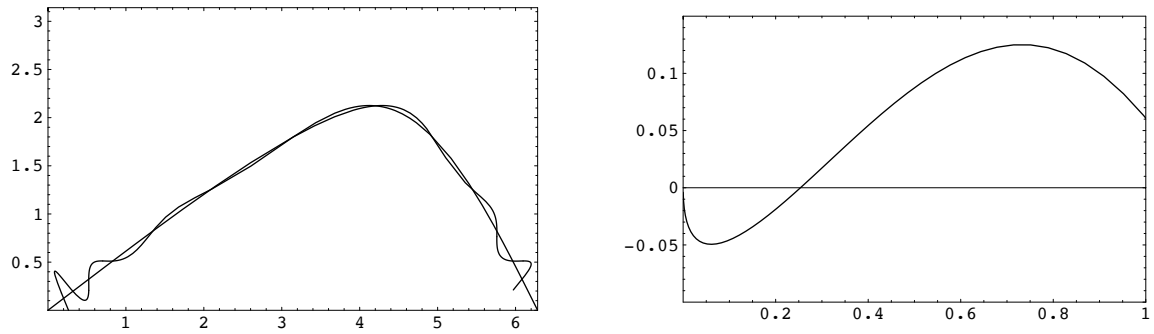

Figure 1: Separatrices of the standard map for $\varepsilon = 1$ (left) and the relative error of the approximation provided by the asymptotic formula (2) plotted against ε (right).

the following asymptotic formula for the angle between the stable and unstable separatrices at the primary homoclinic point:

$$\alpha = \frac{\pi}{\varepsilon}\, \mathrm{e}^{-\frac{\pi^2}{\sqrt{\varepsilon}}} \left(1118.8277059409\ldots + O(\sqrt{\varepsilon})\right). \tag{2}$$

The formula implies that the homoclinic point is transversal but the angle between the separatrices is exponentially small compared to ε. The proof of this asymptotic formula does not provide an explicit estimate on the domain of its validity. Comparing the prediction of the asymptotic formula with numerically computed values of the homoclinic angle, we see that the relative error of the asymptotic formula does not exceed 15% on the full interval $\varepsilon \in (0, 1)$ (see Figure 1). Therefore the asymptotic formula provides a good prediction for the splitting of separatrices even in the region of moderate values of ε, where the splitting of separatrices is visible (like on the left Figure 1).

In order to state and compare the results, it is more convenient to use invariantly defined quantities. In particular, let λ be the largest multiplicator or dominant eigenvalue of the hyperbolic fixed point and $h = \log \lambda$. It is easy to check

$$\varepsilon = 4 \sinh^2 \frac{h}{2},$$

which implies that $h = \sqrt{\varepsilon}\,(1 + O(\varepsilon))$. In this paper we use h as a small parameter instead of ε.

Instead of the homoclinic angle it is more convenient to use a homoclinic invariant ω to measure the splitting of separatrices. The homoclinic invariant is defined as the area of a parallelogram defined by two vectors tangent to the stable and unstable manifolds at a homoclinic point (see (6)). Of course, the area of the parallelogram depends from the length of the tangent vectors. Fortunately, there is a natural way to normalise the tangent vectors in a coordinate independent way. We give a formal definition of the homoclinic invariant in the next section.

The area of lobe formed by segments of stable and unstable separatrices between two adjacent homoclinic points is another popular invariant quantity to consider. We note that in most cases considered in this paper the lobe area equals to $\omega h^2/(2\pi^2)$ up to an exponentially small quantity of higher order. Therefore, the lobe area usually has the same asymptotic expansion as ω up to a simple pre-factor $h^2/(2\pi^2)$. From the numerical point of view, the lobe area is much more difficult to compute.

The homoclinic invariant of the standard map can be represented by the following asymptotic series [5]

$$\omega \asymp \frac{4\pi^2}{h^2}\, \mathrm{e}^{-\frac{\pi^2}{h}} \sum_{k \geq 0} \omega_k h^{2k}\,.$$

The coefficients of these series are defined as solutions of a sequence of parameterless problems. These can be solved numerically to determine the values of each of the coefficients consecutively [6], in particular ω_1 is

the so-called Lazutkin splitting constant:

$$\omega_1 = 1118.827705940900778415146393236018412247147 9\ldots$$

There are no known explicit formulae for the coefficients. Numerical experiments suggest that the asymptotic series is divergent for all $h \neq 0$ and belongs to the Gevrey-1 class:

$$\omega_k \sim A_0 \frac{(2k)!}{(2\pi^2)^{2k}},$$

where $A_0 \approx 1.6275... \cdot 10^6$.

A natural generalisation of the standard map is a map of the form

$$x_1 = x + y_1, \qquad y_1 = y + \varepsilon f(x). \tag{3}$$

Note that the area-preserving Hénon map is a special case, which corresponds to $f(x) = x - x^2$.

The asymptotic behaviour of the homoclinic invariant is very sensitive to the form of the map. The leading term of the asymptotics for the homoclinic invariant is known if f is a trigonometric or algebraic polynomial. On the other hand we do not know a priori the form of an asymptotic expansion excepting the cases of the standard and Hénon maps. We have developed methods suitable for studying the following classes of functions:

- f polynomial
- f trigonometrical polynomial
- f meromorphic or rational function.

We pay special attention to the polynomial case.

In [9] one of the authors provided a conjecture on the form of asymptotic expansions. In this paper we provide a strong numerical evidence which shows that a higher diversity of asymptotic expansions arises in this class of problems, the initial conjecture being the simplest one of this class of expansions.

We summarise the conclusions of our study:

- Asymptotic expansions can be restored up to a high order from direct numerical evaluation of the homoclinic invariant.
- The computational procedure is only stable if the basis of functions of the asymptotic expansion is correct.
- The simple form of an asymptotic expansion $\omega \asymp \mathrm{e}^{-c/h} \sum_{k \geq k_0} c_k h^k$ does not hold for most of the polynomial examples we studied. We found alternative bases for the expansions, which include logarithmic terms and rational powers of h.
- If f is a polynomial of degree n with $n > 4$ then there is an open subset in the space of its coefficients such that the asymptotic expansion for ω oscillates periodically in h^{-1}. Moreover, if $n > 5$ then quasi-periodic oscillations with two rationally independent frequencies is a phenomenon of co-dimension 1 for a generic f.
- In several examples we tested the asymptotic behaviour of the asymptotic coefficients and discovered that they belong to the Gevrey-1 class.

Our computations are based on high-precision computation of the homoclinic invariant for several values of the parameter h and consecutive extraction of coefficient of an asymptotic expansion from this data. These types of results are unachievable using conventional precision. We observed that no reliable conclusion on

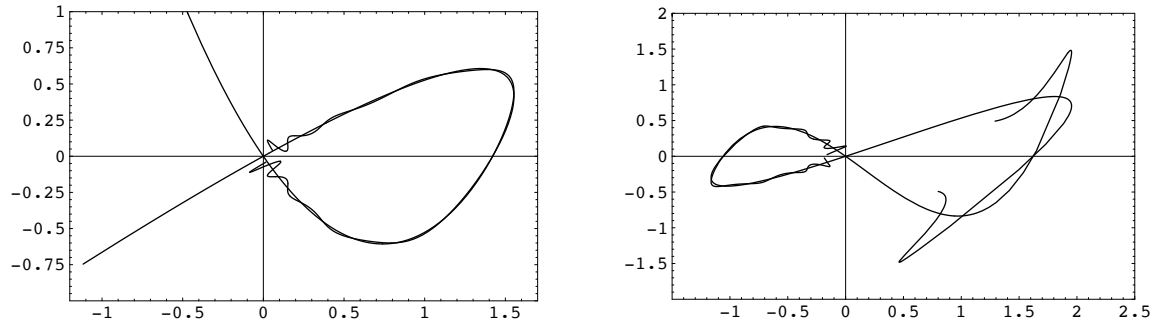

Figure 2: Typical pictures of the stable and unstable separatrices: the quadratic map with $\varepsilon = 1$ (left) and the asymmetric cubic map with $\varepsilon = 0.6$, $r = 0.5$ (right).

the form of an asymptotic expansion can be typically made if the precision of computation is less than 200 decimals.

The rest of the paper has the following structure. In Section 2 we review analytical results on the splitting of separatrices for the generalised standard map. Section 3 describes the numerical methods used. Section 4. provides a detailed description of asymptotic formulae computed for the generalised standard maps with polynomial $f(x)$ of degrees from 2 to 5. Section 5 consists of two parts. First, we give a list of examples, where explicit formulae for the separatrices of the limit flow are available and their singularities are explicitly known. Second, we describe a method to determine the number and position of leading singularities for a polynomial $f(x)$. In the conclusion, we shortly discuss various types of asymptotic behaviour observed in our numerical experiments, which have not been covered in detail in Section 4.

2 Splitting of separatrices for a generalised standard map

We assume that the origin is a hyperbolic fixed point. Without any loss of generality, we may also assume

$$f(0) = 0 \quad \text{and} \quad f'(0) = 1\,.$$

Let $\lambda > 0$ be the largest multiplicator of the fixed point and let $h = \log \lambda$. A direct calculation shows

$$\varepsilon = 4 \sinh^2(h/2).$$

Therefore, $h = \sqrt{\varepsilon}\,(1 + O(\varepsilon))$. We use h as a small parameter for our expansions instead of ε. In most of our experiments the separatrices of the generalised standard map look similar to the ones shown on Figure 2.

The generalised standard map is reversible. The reversor

$$R(x, y) = (x - y, -y)$$

conjugates the generalised standard map to its inverse. There are infinitely many other reversing involutions of the standard map. Indeed, if a map S commutes with the generalised standard map, then $R \circ S$ is a reversor as well. A power of the standard map is an example of S. Moreover, some of the generalised standard maps are odd, and others commute with translations if f is periodic.

The fixed lines of a reversor are called *symmetry lines*. Two of the symmetry lines are given by

$$\ell_0 = \{\, (x, y) \in \mathbb{R} : y = 0 \,\}, \qquad \ell_1 = \{\, (x, y) \in \mathbb{R} : y = -\tfrac{\varepsilon}{2} f(x) \,\}.$$

The first one corresponds to the reversor R.

An intersection of the unstable manifold with a symmetry line is a homoclinic point. We say that a "first" intersection in the internal topology of the invariant manifolds is called *a primary homoclinic point*.

According to this definition there are two different primary homoclinic points, which define two different primary homoclinic trajectories. Most of our computations are done for the homoclinic invariant of the "main" primary homoclinic point on the line ℓ_0.

In order to compute the stable and unstable separatrices of the map, we construct their parametrisation by solutions of the following finite-difference equation of second order:

$$x(t+h) - 2x(t) + x(t-h) = \varepsilon f(x(t)) \tag{4}$$

subject to the following asymptotic condition:

$$x_u(t) = \mathrm{e}^{t} + O(\mathrm{e}^{2t}) \quad \text{as} \quad t \to -\infty \qquad \text{and} \qquad x_s(t) = \mathrm{e}^{-t} + O(\mathrm{e}^{-2t}) \quad \text{as} \quad t \to +\infty, \tag{5}$$

respectively. The y-component of the separatrix is restored by $y_u(t) = x_u(t) - x_u(t-h)$.

The asymptotic condition fixes the functions $x_u(t)$ and $x_s(t)$ uniquely. Moreover, if $x(t)$ satisfies equation (4), then $x(-t)$ do it as well. Taking into account the asymptotic condition, we get $x_s(t) = x_u(-t)$.

Let γ_0 be a homoclinic point, then there exist t_u and t_s such that

$$x_u(t_u) = x_s(t_s) \qquad \text{and} \qquad y_u(t_u) = y_s(t_s).$$

We define two vectors tangent to W^u and W^s at γ_0 by

$$e_u = (\dot{x}_u(t_u), \dot{y}_u(t_u)) \qquad \text{and} \qquad e_s = (\dot{x}_s(t_s), \dot{y}_s(t_s)).$$

The homoclinic invariant is defined as the area of a parallelogram defined by the two tangent vectors:

$$\omega = \Omega(e_u, e_s), \tag{6}$$

where $\Omega = dx \wedge dy$ is the standard area form. The generalised standard map preserves area and consequently ω takes the same value for every point of the trajectory of γ_0. Moreover, ω is invariant with respect to symplectic coordinate changes, which allows direct comparison of results for a map written in different coordinates. The angle between W^u and W^s at γ_0 can be found by

$$\alpha = \sin^{-1} \frac{\omega}{\|e_u\| \, \|e_s\|}.$$

Therefore if $\omega \neq 0$ the intersection is transversal.

Naturally, equation (4) can be considered as a finite-difference approximation of the differential equation

$$\ddot{x}_0 = f(x_0)\,. \tag{7}$$

Note that deriving this equation we used that $\lim_{h\to 0} \varepsilon h^{-2} = f'(0) = 1$.

Let x_0 be a separatrix solution of equation (7). There is a constant $\rho > 0$ such that $x_0(t)$ is analytic for $t \in \Pi_\rho = \{\, t \in \mathbb{C} : |\Im t| < \rho \,\}$ and has singularities on the boundary of this strip. The position and type of the singularities determine [3] the asymptotic behaviour of the homoclinic invariant ω for small $h > 0$. We say that these are the *leading singularities*.

Let us assume that the separatrix of the differential equation intersects the line $y = 0$ at $t = 0$: $\dot{x}_0(0) = 0$. Then x_0 is even due to the symmetry of the differential equation. This also follows from the Hamiltonian $\frac{1}{2}y^2 - F(x)$, where F is a primitive of f, associated to equation (7).

Since x_0 is even and real-analytic, we conclude that if $t_* = \beta + \mathrm{i}\rho$ is a singular point then $\pm\beta \pm \mathrm{i}\rho$ are singular points as well. Hence, it is enough to consider leading singularities on the upper component of the boundary of the strip Π_ρ. We should expect that in a generic situation there is either one leading singularity at the point $\mathrm{i}\rho$ or two singularities at the points $\mathrm{i}\rho \pm \beta$. The cases of co-dimension one are expected to have either 3 or 4 leading singularities.

Let $f(x) = \sum_{k=1}^{n} f_k x^k$ be an algebraic polynomial of degree n. We assume that

$$f_1 = 1 \qquad \text{and} \qquad f_n < 0.$$

n	$\lvert\Theta(n)\rvert$
2	2,474,425.59355325105384085474952801975649807563783 88
3	7,964.37391517522220406901069341740362179385258 84
4	930.15334750194623088774196558589820660431268 14
5	279.56330397398077310037795608276394847337699 48
6	125.29043795369955323870255174439429750930423 10

Table 1: Numerical values of the splitting constants for polynomial maps of degrees from 2 to 6.

Consider the following two auxiliary constants:

$$\nu = \frac{2(n+1)}{n-1} \qquad \text{and} \qquad d = |f_n|^{\nu/2}.$$

In [4][1] it was shown that

- in the case of one leading singularity $\mathrm{i}\rho$

$$\omega = \frac{4\pi|\Theta(n)|}{dh^\nu}\,\mathrm{e}^{-2\pi\rho/h} + \dots$$

- in the case of two leading singularities at $\mathrm{i}\rho \pm \beta$

$$\omega = \frac{8\pi|\Theta(n)|}{dh^\nu}\,\mathrm{e}^{-2\pi\rho/h}\cos\left(\frac{2\pi\beta}{h} + \varphi\right) + \dots$$

- in the case of three leading singularities $\mathrm{i}\rho \pm \beta$ and $\mathrm{i}\rho$

$$\omega = \frac{4\pi|\Theta(n)|}{dh^\nu}\,\mathrm{e}^{-2\pi\rho/h}\left(1 + 2\cos\left(\frac{2\pi\beta}{h} + \varphi\right)\right) + \dots$$

- in the case of four leading singularities at $\mathrm{i}\rho \pm \beta_1$ and $\mathrm{i}\rho \pm \beta_2$

$$\omega = \frac{8\pi|\Theta(n)|}{dh^\nu}\,\mathrm{e}^{-2\pi\rho/h}\left(\cos\left(\frac{2\pi\beta_1}{h} + \varphi_1\right) + \cos\left(\frac{2\pi\beta_2}{h} + \varphi_2\right)\right) + \dots$$

The asymptotic formulae contain the constants $|\Theta(n)|$ and the phases

$$\varphi, \varphi_1, \varphi_2 \in \left\{ \frac{2\pi k}{n-1} : k \in \mathbb{Z}_{n-1} \right\}.$$

The constants $\Theta(n)$ are complex constants defined using the parameter free maps [6]

$$(x, y) \mapsto (x_1, y_1), \qquad x_1 = x + y_1, \quad y_1 = y + x^n\,.$$

They do not have any known expressions in terms of fundamental constants. We note that the numerical evidence suggests $\arg\Theta(n) = -\frac{\pi}{2} + \frac{2\pi}{n-1}$ although there is no analytical proof of this for $n \neq 2$.

The numerical values for $|\Theta(n)|$ have been computed numerically by a method described in [6] and are given in Table 1. These computations were performed with 1000 correct digits and used in testing the correctness of other numerical results.

[1] The phases φ_k are missing in that paper. In the case of a trigonometrical polynomial f the phases vanish.

3 Numerical methods

Our numerical procedure consists of two main steps. First we compute the values of the homoclinic invariant for the parameter h on a subinterval of $(0,1)$. The precision of these computations is typically in the range from 200 to 1500 correct digits. Then we use these data to extract coefficients of an asymptotic expansion. We note that the asymptotic series are typically divergent. Moreover, in most cases we do not have a rigorous proof of the correctness of the form of the asymptotic expansion, so special attention should be given to validation of the results.

3.1 Computation of the homoclinic invariant

Our method is based on the definition (6). We designed a procedure which computes a point on W^u and a vector tangent to W^u at that point using the parametric representation based on equation (4). Then we use Newton's method to find the first intersection of W^u with the symmetry line ℓ_0. This is the main primary homoclinic point. We obtain a vector e_s tangent to W^s at that point applying the reversor to $-e_u$.

Now we give more details on the procedure used in computations of W^u. It is convenient to make the substitution $z = \mathrm{e}^t$. Then $z = 0$ corresponds to the fixed point. Equation (4) takes the form

$$x(\lambda z) - 2x(z) + x(\lambda z) = \varepsilon f(x(z)) \tag{8}$$

and can be solved using power series

$$x(z) = \sum_{k=1}^{\infty} c_k z^k.$$

The series converge in a disk, which can be chosen independent from ε (see [3]). Moreover, if f is entire the radius of convergence is infinite. Consider the Taylor series of f

$$f(x) = \sum_{k=1}^{\infty} f_k x^k.$$

The coefficient c_1 is not determined by the equation, but the asymptotic condition (5) suggests c_1=1. A direct substitution of the series into the equation (8) leads to a recurrent system on the coefficients c_k, which can be easily solved: let $Y_{1,1} = a_1$, and compute the coefficients of $x(z)$ by evaluating

$$\begin{aligned} Y_{m,i} &= \sum_{k=i-1}^{m-1} Y_{k,i-1} c_{m-k} \qquad i = 2, \ldots, m, \\ c_m &= \frac{\varepsilon}{\lambda^m + \lambda^{-m} - 2 - \varepsilon f_1} \sum_{i=2}^{m} Y_{m,i} f_i, \\ Y_{m,1} &= c_m \end{aligned}$$

consecutively for $m \geq 2$. The auxiliary functions $Y_{i,m}$ are Bell's polynomials.

In the actual computations, we chose the number of terms M and the number of iterates N and compute an approximation to a point on the local unstable manifold by computing first the point

$$x_{-N} = \sum_{k=1}^{M} c_k \mathrm{e}^{k(t-Nh)}, \qquad x_{-N-1} = \sum_{k=1}^{M} c_k \mathrm{e}^{k(t-h-Nh)}.$$

and a tangent vector

$$e_{-N} = \sum_{k=1}^{M} k c_k \mathrm{e}^{k(t-Nh)}, \qquad e_{-N-1} = \sum_{k=1}^{M} k c_k \mathrm{e}^{k(t-h-Nh)}$$

and then iterating the equations N times:

$$\begin{aligned} x_{n+1} &= 2x_n - x_{n-1} + \varepsilon f(x_n), \\ e_{n+1} &= 2e_n - e_{n-1} + \varepsilon f'(x_n)e_n. \end{aligned}$$

We restore the y component to get the point $\gamma_h = (x_0, x_0 - x_{-1})^T \in W^u$ and the tangent vector $e_u = (d_0, d_0 - d_{-1})^T \in T_{\gamma_h} W^u$.

It is convenient to use optimisation on M, N as a function of h to minimise the computational effort, specially for small h. The number of decimal digits to be used can be obtained from a priori estimates on the value of $\omega(h)$ and the relative error desired for $\omega(h)$ to be able to obtain accurate coefficients of an asymptotic expansion. If M is small, the local representation is only accurate on a small interval. This increases the value of N and the cost of the iterates. But a too large value of M, which decreases N, increases the cost of the computation of the c_k coefficients. It is also clear that not all the c_k are needed with the same number of digits and that the number of digits needed in Newton's method roughly doubles at each Newton iterate. All these considerations allow to decrease the computing time in a significative way.

Now assume, for definiteness, that the configuration of separatrices is like the one shown on Figure 2. Then the main primary homoclinic point is the first intersection of W^u with $y = 0$. In order to find a homoclinic point we apply Newton's method to solve the equation $y(t) = 0$, which is equivalent to $x(t) = x(t - h)$. The tangent vector to W_s is obtained by applying the reversor R to $-e_u$, and the homoclinic invariant is finally evaluated by the formula:

$$\omega = d_0^2 - d_1^2 \,.$$

A similar formula can be derived for the standard map with $f(x) = \sin(x)$, where the configuration of separatrices is different, and the main primary homoclinic point belongs to a different symmetry line, namely to $x = \pi$.

3.2 Obtaining coefficients of an asymptotic expansion

We choose a short interval $I_1 \subset (0, 1)$, where the homoclinic invariant is typically of order 10^{-1500}—10^{-500}, and for a finite subset of points we compute the homoclinic invariant using the procedure described in the previous section. Then we normalise it using the formula

$$\hat{\omega}(h) = \frac{dh^\nu}{4\pi} \, \mathrm{e}^{2\pi\rho/h} \omega(h) \,.$$

In the case of a non-oscillating asymptotic and a polynomial f, the normalisation implies $\hat{\omega}(h) \to |\Theta(n)|$ when $h \to 0$. We reconstruct coefficients of the asymptotic expansion by fitting its partial sums to the data. On this stage we use as many points as the number of unknown coefficients. Therefore the best fitting produces an interpolating function.

Of course, this procedure will produce coefficients for any asymptotic basis of functions, independently of the true asymptotic behaviour of the homoclinic invariant.

In all cases studied in this paper excepting the standard map and Hénon map, the form of the asymptotic expansion is not known a priory and a part of the problem is to chose an asymptotic basis correctly. We use a complex matching method to guess potentially suitable candidates. In order to test correctness of our choice we perform three tests:

- Numerical stability test: computations involving different partial sums and different sets of data should lead to essentially the same values for the coefficients.
- Extrapolation to zero: the first term of the computed series has to coincide with the a priori known leading term described in the previous section. In this test we compare the result of interpolation with the independently computed constants $|\Theta(n)|$.

- Extrapolation to the interval $(0,1)$: the difference between $\hat{\omega}(h)$ and a partial sum of the series should behave in a way compatible with the definition of asymptotic expansion, i.e., it should be of order of the "first omitted term" within expected precision of computation.

The last two tests rely on the well known observation that in general an interpolating function does not have good extrapolation properties and therefore it should fail the tests. If an asymptotic basis is not properly chosen, we typically see that the differences between $\hat{\omega}$ and the partial sum increase rapidly on both sides of I_1. Meanwhile, the asymptotic expansion provides an excellent approximation on the whole interval $(0,1)$ with errors decreasing with h.

In these experiments we mostly use h in an interval around 10^{-3} or 10^{-2} and evaluate $\hat{\omega}(h)$ with 200—1500 correct digits. We remark that smaller values of h are inaccessible because the number of digits necessary to compute $\omega(h)$ with a given precision grows exponentially in h^{-1} due to the exponential smallness of $\omega(h)$.

Typically we see that a successful choice of the asymptotic basis allows us to pass the first two tests with precision in the region of 10^{-50}—10^{-900}. At the same time an incorrect ansatz for the asymptotic expansion is unable to produce errors less than 10^{-10}.

4 Examples

4.1 Hénon map

The area-preserving Hénon map is obtained as a particular case of (3) when $f(x) = x - x^2$. It has a hyperbolic fixed point at the origin and there is a primary homoclinic point at the intersection of the separatrices with the positive semiaxis of the variable x. The homoclinic invariant at this point can be represented by an asymptotic series in even powers of h [6]:

$$\omega_0(h) \asymp \frac{4\pi}{h^6} e^{-2\pi^2/h} \sum_{k\geq 0} a_k h^{2k}. \tag{9}$$

In our first set of numerical experiments we computed around 280 coefficients a_k and examined their behaviour for large k. In order to achieve this, we computed the primary homoclinic point and two vectors e_u and e_s tangent to the stable and unstable separatrix at this point. Then we computed the homoclinic invariant $\omega_0(h)$ and normalised it by considering

$$\hat{\omega}_0(h) = \frac{h^6}{4\pi} e^{2\pi^2/h}\ \omega_0(h).$$

The asymptotic expansion (9) is equivalent to

$$\hat{\omega}_0(h) \asymp \sum_{k\geq 0} a_k h^{2k}. \tag{10}$$

We note that the leading term of this asymptotic expansion is known with an extremely high precision of several thousands decimals obtained from an independent numerical experiment. The first digits of this constant are provided in Table 1 ($n = 2$).

The behaviour of the function $\hat{\omega}_0(h)$ is illustrated by Figure 3. We see that the leading term of the asymptotic formula (10) predicts the value of the separatrix splitting with a reasonable accuracy not only for very small but also for moderate values of h.

We computed $\hat{\omega}_0(h)$ with 1600 correct digits for 300 points uniformly distributed in the interval $h \in I_0 = [\frac{3}{1000}, \frac{6}{1000}]$. Then we chosen a number N and constructed an interpolating polynomial $\sum_{k=0}^{N} \tilde{a}_k h^{2k}$ to fit the first $N+1$ of those points. We used the three tests described in the previous section to control the accuracy of our computations.

For the subsequent analysis we used only coefficients which showed a reasonable numerical stability to changes of the parameters of the experiment (more than 40-50 stable digits). The stability is extremely good for the first coefficients a_k (from 500 to 900 decimal digits) and then gradually decreases when k grows.

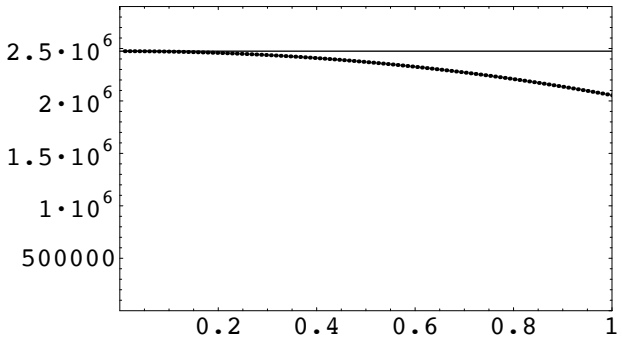

Figure 3: Hénon map: Normalised homoclinic invariant $\hat{\omega}_0$ plotted as a function of h. The horizontal line corresponds to the prediction based on the leading term of the asymptotic formula (10) solely.

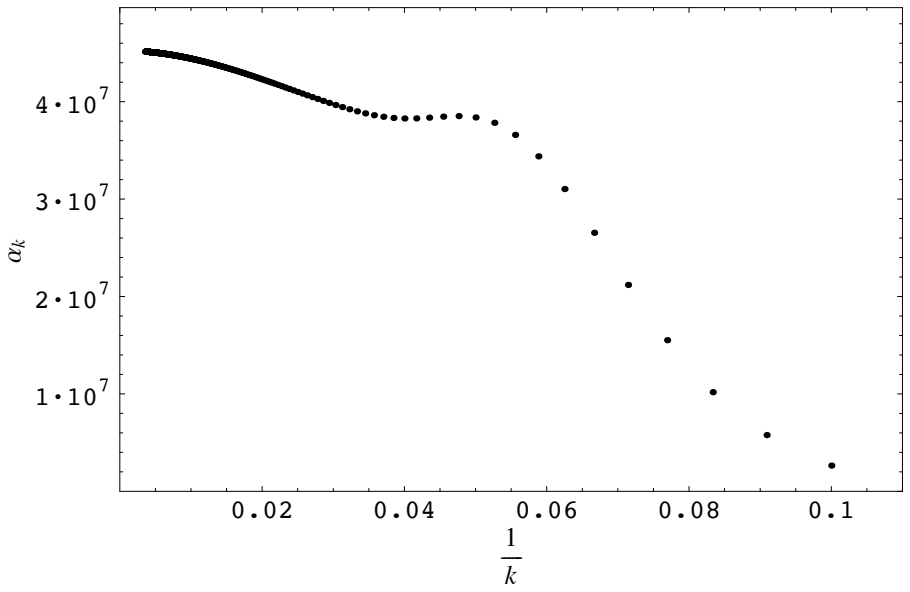

Figure 4: Hénon map: Normalised coefficients of the asymptotic expansion (10), $\hat{a}_k = a_k \left(\frac{(2k+6)!}{(4\pi^2)^{2k}}\right)^{-1}$, plotted as a function of k^{-1} for $k \geq 10$.

The first coefficient of the asymptotic series is positive and it is followed by 8 negative ones: $a_k < 0$ for $1 \le k \le 8$. All other coefficients are again positive. We conjecture the following asymptotic behaviour for large k:

$$a_k \sim A_0 \frac{(2k+6)!}{(4\pi^2)^{2k}}.$$

The dependence of the ratio $\hat{a}_k := a_k / \left(\frac{(2k+6)!}{(4\pi^2)^{2k}}\right)$ on k^{-1} is shown on Figure 4, which clearly indicates that a limit of $\hat{a}_k$ for $k^{-1} \to 0$ may exist. The convergence to the limit seems to be polynomial in k^{-1}: $\hat{a}_k = A_0 + O(k^{-2})$. We use an extrapolation technique based on polynomial expansions in powers of k^{-1} to get an estimate for the limit value:

$$A_0 = 4.525469045029776536 19 \cdot 10^7.$$

Note that without extrapolation nor more than 2-3 correct digits of A_0 could be seen.

In this way, we have got strong numerical evidence in support of the following conjectures.

- The asymptotic series (10) are of Gevrey-1 type with respect to h.
- The corresponding Borel transform is analytic in a disk of the radius $4\pi^2$ centred at the origin. On the boundary of the disk there are two singularities at $\pm 4\pi^2$. The leading order of the singularities of the Borel transform are poles.

Next, we study the deviation of the homoclinic invariant from its asymptotic expansion. Gevrey-1 series diverge in general and several summations methods are available. We use the most naive method called "the astronomers recipe", which uses partial sums to evaluate a divergent series. Following the recipe, we define

$$\hat{\omega}_{\mathrm{astr}}(h) = \sum_{k=0}^{M(h)-1} a_k h^{2k},$$

where $M(h)$ corresponds to the term $a_k h^{2k}$, which has the smallest absolute value. The asymptotic behaviour of a_k combined with Stirling's formula implies that for small h we get $M(h) \approx 2\pi^2/h$. Moreover, the smallest term is of the order of $\mathrm{e}^{-2M(h)}$ or, equivalently, $\mathrm{e}^{-4\pi^2/h}$. The value of $\hat{\omega}_{\mathrm{astr}}(h)$ jumps when $M(h)$ changes its value. We can interpret the jumps as uncertainty of the summation method. This uncertainty is of the order of the first skipped term. Therefore the astronomers recipe evaluates the asymptotic series (10) with an uncertainty of the order of $\mathrm{e}^{-4\pi^2/h}$.

We computed the values of $\hat{\omega}_0(h)$ with 600 correct digits for several hundreds points from the interval $h \in (\frac{4}{100}, \frac{10}{100})$. We discovered that $\hat{\omega}_0(h) - \hat{\omega}_{\mathrm{astr}}(h)$ decreases approximately as an exponential function $b_0 \mathrm{e}^{-2\pi^2/h}$, which is exponentially larger than the uncertainty in the evaluation of $\hat{\omega}_{\mathrm{astr}}(h)$. Then we extracted coefficients of an asymptotic expansion for $\hat{\omega}_0(h) - \hat{\omega}_{\mathrm{astr}}(h)$ following procedures similar to the already described. This enabled us to reliably extract around 25 coefficients of the series

$$\hat{\omega}(h) - \hat{\omega}_{\mathrm{astr}}(h) \asymp \mathrm{e}^{-2\pi^2/h} \sum_{k \ge 0} b_k h^{2k}.$$

In particular, the leading coefficient was found with precision of around 50 digits:

$$b_0 = -5.2204595407324285706\ldots \cdot 10^{11}.$$

We conclude the homoclinic invariant of the Hénon map can be expanded in a hyper-asymptotic expansion, which contains exponentially small terms of two different orders:

$$\omega_0 = \frac{4\pi}{h^6} \mathrm{e}^{-2\pi^2/h} \left(\sum_{k \ge 0} a_k h^{2k} + \mathrm{e}^{-2\pi^2/h} \sum_{k \ge 0} b_k h^{2k} \right),$$

We used partial sums of this expansion to predict values of ω_0 for moderate values of $h \in (0,1)$. First, we numerically observed that the relative error of approximating $\hat{\omega}(h)$ by $\hat{\omega}_{\rm astr}(h)$ alone does not exceed 10^{-3} for $h \in (0,1)$ and rapidly decreases with h. Taking into account the second exponent, we substantially improved the precision of the approximation for $h < 0.7$. On the other hand, we observed that the inclusion of the second exponent increased the approximation error for larger h.

In the case of the Hénon map, exponentially small terms of higher exponential order (that is, powers of $\mathrm{e}^{-2\pi^2/h}$) have been detected but their inclusion into the hyper-asymptotic expansion does not increase the domain where the asymptotic expansion accurately predicts the values of the homoclinic invariant.

The Hénon map has two distinct primary homoclinic trajectories. The second one contains an intersection of the separatrices with the second symmetry line ℓ_1 given by $y = -\frac{\varepsilon}{2}(x - x^2)$. The asymptotic expansion for the second primary homoclinic trajectory ω_1 differs only by the minus sign in front of the asymptotic series. In spite of having the common asymptotic expansion, $\omega_0 \neq -\omega_1$. Our numerical experiments showed that $\omega_0 + \omega_1$ is an exponentially small quantity of the second exponential order:

$$\omega_1 + \omega_2 \asymp \frac{8\pi}{h^6} e^{-4\pi^2/h} \sum_{k\geq 0} c_k h^{2k}.$$

We computed around 100 coefficients of this expansion. It is interesting to remark that $c_k = b_k$ within the precision of our computation for all k, when both coefficient are known. The reason for this coincidence is unknown to us, but one can conjecture that while the dominant exponentially small terms are related to a "first order variational" behaviour around W^u, W^s, changing sign at both primary homoclinic points, the terms in $e^{-4\pi^2/h}$ collect the contribution of "second order variationals" and are equal at both points.

4.2 Cubic map

4.2.1 Symmetric case

Our study of the generalised standard map (3) with $f(x) = x - x^3$ leads to conclusions similar to the case of the Hénon map. The homoclinic invariant of the main homoclinic orbit is given asymptotically by

$$\omega_0(h) \asymp \frac{4\pi}{h^4} e^{-\pi^2/h} \sum_{k\geq 0} a_k h^{2k},$$

where the leading coefficient $a_0 = -|\Theta(3)|$ (see Table 1). Similar to the cases of the Hénon map and the standard map the asymptotic expansion contains only even power of h.

Unlike the standard map, in the present case there is no proof of the validity for this asymptotic expansion. On the other hand, our numerical evidence suggests that the method described in [5] can be used without any major modification due to the similarity in the properties of the asymptotic expansions.

We computed 250 coefficients of the expansion to discover that $a_0 = -|\Theta(3)|$ within the 800 first digits. The asymptotic behaviour of the coefficients a_k for large k is not exactly the same as in the case of the Hénon map but very similar

$$a_k \sim A_0 \frac{(2k+4)!}{(2\pi^2)^{2k}} \qquad \text{with } A_0 = 183645.251245264885\ldots$$

The series are also of Gevrey-1 type and the radius of convergence of the Borel transform is $2\pi^2$, which coincides with $4\pi\rho$, where $\rho = \frac{\pi}{2}$ is the width of the analyticity strip for the separatrix of the limit flow $\ddot{x}_0 = x_0 - x_0^3$. This relation between the radius of convergence and the position of the separatrix singularity remains the same for all examples when we were able to compute the radius.

4.2.2 Asymmetric case

In the case of a generic polynomial of degree 3, the asymptotic behaviour of the homoclinic invariant is different from the one described above. If the separatrices of the limit flow form a figure "eight" the corresponding function f can be normalised to $f(x) = x + rx^2 - x^3$ for some $r \in \mathbb{R}$. If $r = 0$ we get the symmetric case described in the previous subsection. It is easy to see that the substitution $x \mapsto -x$ is equivalent to $r \mapsto -r$, and instead of studying the right loop for all r we may study both the right and left loops for $r \geq 0$.

The separatrices of the limit flow are explicitly known and described in Section 5.1. It is interesting to note that the heights of the complex singularities for the right and left loops are different and equal to

$$\rho = \cot^{-1} \frac{r\sqrt{2}}{3} \qquad \text{and} \qquad \pi - \rho,$$

respectively. Since $r > 0$ the right loop is larger than the left one, and its leading singularity is closer to the real axis. Consequently in the case of an asymmetric cubic map, the splitting of separatrices to the right of the origin is exponentially small compared to h but simultaneously it is exponentially large compared to the splitting of separatrices on the left hand side. This phenomenon can be easily observed on Figure 2 (right). In the absence of a symmetry different asymptotic behaviour of the left and right separatrix whiskers is typical and should be observed in a generic situation.

In fact, if we consider an area-preserving map around an elliptic fixed point, together with the chain of islands which occur in a resonance zone, there is a hyperbolic periodic orbit which gives rise to "inner" and "outer" splittings. Inner ones are associated to the primary homoclinics which occur closer to the elliptic point than the chain of islands, while the outer ones are related to primary homoclinics which are found outside the chain of islands. The differences in the splittings are due to the changes in the rotation number (of an integrable approximation) along the resonance zone. Close to the elliptic point these changes are related to the second Birkhoff coefficient of the Normal Form around the elliptic fixed point. See [10], specially Appendix A, for details.

As before we introduce now the normalised homoclinic invariant by

$$\hat{\omega}(h) = \frac{h^4}{4\pi} \mathrm{e}^{2\pi\rho/h}\, \omega(h). \tag{11}$$

Fixing a value for the parameter r, it is easy to check numerically that $\hat{\omega}(h)$ is rather close to $|\Theta(3)|$ for small values of h. Nevertheless all our attempts to apply the interpolation method to compute coefficients of asymptotic expansions in the form of a power series in h^2 or h have failed due to an obvious lack of numerical stability and extrapolability properties. This indicates that $\hat{\omega}(h)$ does not have an asymptotic expansion in the form of a power series.

We repeated the procedure taking $\log \hat{\omega}(h)$ instead of $\hat{\omega}(h)$. Our numerical computation suggests that

$$\log \hat{\omega}(h) \asymp \sum_{k\geq 0} a_k h^k + \log h \sum_{k\geq 0} b_k h^{2k}\,. \tag{12}$$

We tested this form of expansion for several different values of the parameter $r > 0$. Here we present the results for $r = \frac{1}{2}$ as a typical example.

We computed the coefficients up to order 70 in h by fitting the coefficients to the directly computed values of $\log \hat{\omega}(h)$. We observed that in our best experiments $a_0 - \log|\Theta(3)|$ was of the order of 10^{-270} while using $h \in I_1 = (\frac{3}{1000}, \frac{5}{1000})$. This means that using this asymptotic basis the extrapolation from the interval I_1 to 0 produces a result which coincides in its first 270 digits with the analytical prediction obtained with a completely independent evaluation of $|\Theta(3)|$. This is quite a strong indication that the proposed form of the expansion is correct.

For large k, the coefficients grow rapidly and we use the normalisation

$$\hat{a}_k = \frac{(4\pi\rho)^k}{(k+4)!} a_k\,.$$

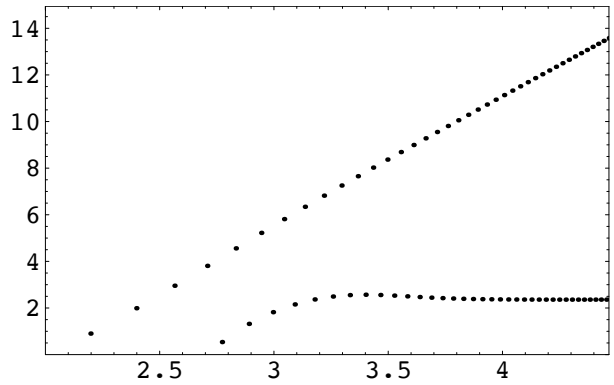

Figure 5: Cubic map with $r = 1/2$: Logarithm of normalised coefficients of the asymptotic expansion, $\log \hat{a}_k$, plotted as a function of $\log k$. The behaviour is different for even and odd values of k.

We see that odd and even coefficient grow at different pace, see Figure 5. The even coefficients behave similar to the symmetric case and odd coefficients grow faster but in a way consistent with the conjecture on the radius of convergence of the Borel transform. The coefficients b_k are essentially of the same order as a_{2k}.

The equations (12) and (11) imply that the homoclinic invariant has an asymptotic expansion of the form

$$\omega(h) = -\frac{4\pi}{h^4} \mathrm{e}^{-2\pi\rho/h} \sum_{k,j\geq 0} c_{kj} h^{k+2j} (\log h)^j, \tag{13}$$

where $c_{00} = |\Theta(3)|$. A direct computation of this series is very difficult numerically because the number of terms of order less than N grows quadratically in N making the numerical procedures much less stable.

4.3 Quartic map

We consider a quartic polynomial of the form

$$f(x) = x + c_2 x^2 + c_3 x^3 - x^4.$$

Let x_0 be the separatrix solution of $\ddot{x}_0 = f(x_0)$ normalised for definiteness by $\dot{x}_0(0) = 0$. As said in section 2 the function x_0 is even in t. We do not know an explicit formula for x_0 (it involves hyperelliptic integrals) except for some special values of the coefficients c_2 and c_3. We consider the function

$$F(x) = \int_0^x f(y)dy.$$

We know three of its five zeroes: $F(0) = F'(0) = F(x_0(0)) = 0$. Let us assume that the other two zeroes are not real, i.e. $F(r\mathrm{e}^{\pm \mathrm{i}\phi}) = 0$ for some $r > 0$ and $\phi \in (0, \pi)$. This domain in r, ϕ is diffeomorphic to an open domain in the c_2, c_3 coefficients. The function F takes the form

$$F(x) = -\frac{x^2}{5}(x^2 - 2r\cos(\phi)x + r^2)\left(x - \frac{5}{2r^2}\right).$$

We note that $x_0(0) = \frac{5}{2r^2}$ due to the normalisation of $f(x)$. Then the singularities of x_0 are given by the integral

$$t_* = \int_\Gamma \frac{dx}{\sqrt{2F(x)}}$$

where the curve Γ goes from $x_0(0)$ to infinity avoiding other zeroes of $F(x)$. The integral depends on the homotopy class of the curve Γ. We will evaluate the integral numerically along a properly chosen straight line. We discuss the problem of choosing Γ in Section 5.2. Here we provide a summary of our study on the leading singularities of x_0:

- There is a constant ρ, $0 < \rho \leq \pi$, such that x_0 is analytic in the strip $|\Im t| < \rho$.
- x_0 has at most 3 singular points on the line $\Im t = \rho$.
- The singularities are branching points of order $-1/3$.
- If $r \in \left(0, \frac{\sqrt[3]{15}}{2}\right]$, there is a single singularity on the line $\Im t = \rho$ at the point $\mathrm{i}\rho$.
- There is a function $\varphi_{\mathrm{cr}} : \left[\frac{\sqrt[3]{15}}{2}, +\infty\right) \to \left(0, \frac{\pi}{2}\right)$ such that
  1. if $\phi > \varphi_{\mathrm{cr}}(r)$, then x_0 has a single leading singularity at $\mathrm{i}\rho$.
  2. if $0 < \phi < \varphi_{\mathrm{cr}}(r)$, then x_0 has a pair of leading singularities at $\mathrm{i}\rho \pm \beta$. In this case $\rho = \pi$ and $\beta = \beta(r) > 0$.
  3. if $\phi = \varphi_{\mathrm{cr}}(r)$ then x_0 has three leading singularities at $\mathrm{i}\pi$ and $\mathrm{i}\pi \pm \beta$. In this case $\rho = \pi$ and $\beta = \beta(r) > 0$.

In particular we see that the situation with two leading singularities is realised on an open subset of parameters, and the situation with three leading singularities is of co-dimension 1. We expect to see asymptotically monotonic behaviour of the homoclinic invariant in the case 1) and asymptotically periodic (in h^{-1}) oscillations in the cases 2) and 3). The function $\varphi_{\mathrm{cr}}(r)$ can be computed numerically (see Figure 6). We see that the graph of this function separates two subsets of parameters, which correspond to monotonic and oscillatory behaviour of the homoclinic invariant.

Next we present several special cases of the quartic map which exhibit different typical types of asymptotic behaviour.

First we consider the simplest case $f(x) = x - x^4$. In this case the separatrix is known explicitly (see Table 2) and $\rho = \frac{\pi}{3}$. The behaviour of the asymptotic expansion is very similar to the cases of the Hénon, standard and symmetric cubic maps. We defined the normalised homoclinic invariant by

$$\hat{\omega}(h) = \frac{h^{10/3}}{4\pi} \mathrm{e}^{2\pi^2/(3h)} \omega(h).$$

Our numerical computations suggest the asymptotic expansion

$$\hat{\omega}(h) \asymp \sum_{k \geq 0} a_h h^{2k},$$

which is confirmed by the extrapolation to zero test passed within the first 500 digits of a_0. The series is Gevrey-1 in h with radius of convergence for the Borel transformed series equal to $4\pi\rho = 4\pi^2/3$.

Non-oscillating asymptotic. Now we let $r = \frac{3}{2}$ and $\phi = \frac{2\pi}{3}$, which is equivalent to the choice

$$f(x) = x - \frac{7}{20}x^2 - \frac{14}{45}x^3 - x^4\,.$$

The leading singularity of x_0 is at $\mathrm{i}\rho$ with $\rho = 1.24747447943895\ldots$ We consider the normalised homoclinic invariant

$$\hat{\omega}(h) = \frac{h^{10/3}}{4\pi} \mathrm{e}^{2\pi\rho/h} \omega(h). \tag{14}$$

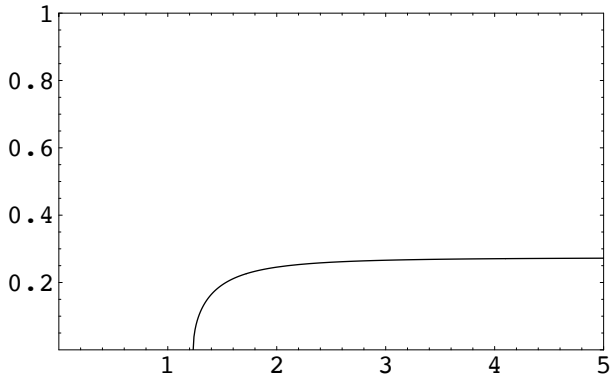

Figure 6: Quartic map: bifurcation of the number of leading singularities on the (r, ϕ)-plane.

Our numerical computations suggest the asymptotic expansion is of the form

$$\hat{\omega}(h) \asymp a_0 + \sum_{k\geq 3} a_k h^{k/3},$$

which contains non-integer powers of h. The form of the expansion is confirmed by the extrapolation to zero test passed within the first 75 digits of a_0.

In all our experiments, where the positions of the leading singularity is not known exactly, we use Mathematica package to evaluate the corresponding integral numerically. Unfortunately, it is not able to do this with a precision higher than approximately 240 correct decimals. This restricts the precision of computation of $\hat{\omega}_0$ and, as a consequence, the number of terms in the asymptotic series we can obtain.

We also observed a curious behaviour in the expansion

$$\log \hat{\omega}(h) \asymp \log a_0 + \sum_{k\geq 3} b_k h^{k/3}.$$

Since $a_0 > 0$, this expansion is equivalent to the expansion for $\hat{\omega}$. The form of the expansions is the same, but we observed that some of the coefficients b_k vanish. Namely, among the reliably computed coefficients up to order 33 we see that

$$b_k = 0 \quad \text{for} \quad k \in \{\, 1, 2, 5, 7, 11, 13, 17, 19, 23, 25, 29, 31 \,\}$$

which, skipping the index $k = 2$, has differences between consecutive values of k equal to 4 and 2 alternatively.

Oscillating asymptotic with $\phi < \varphi_{\mathrm{cr}}$. Now we keep $r = \frac{3}{2}$ and let $\phi = \arccos \frac{9}{10}$, which is equivalent to the choice

$$f(x) = x - \frac{63}{20}x^2 + \frac{686}{225}x^3 - x^4\,.$$

The leading singularities of x_0 are at $\mathrm{i}\pi \pm \beta$ with $\beta = 3.77654795\ldots$ We consider the normalised homoclinic invariant (14). In order to facilitate the comparison of different oscillatory regimes, we additionally divide $\hat{\omega}$ by the constant $|\Theta(4)|$. Our numerical computations suggest the asymptotic expansion

$$\frac{\hat{\omega}(h)}{|\Theta(4)|} \asymp 2\cos\left(\frac{2\pi\beta}{h} + \frac{2\pi}{3}\right) + \cos\left(\frac{2\pi\beta}{h} + \frac{2\pi}{3}\right)\sum_{k\geq 4} a_k h^{k/3} + \sin\left(\frac{2\pi\beta}{h} + \frac{2\pi}{3}\right)\sum_{k\geq 3} b_k h^{k/3}\,. \qquad (15)$$

Both amplitudes are represented by asymptotic expansions which contain powers of $h^{1/3}$.

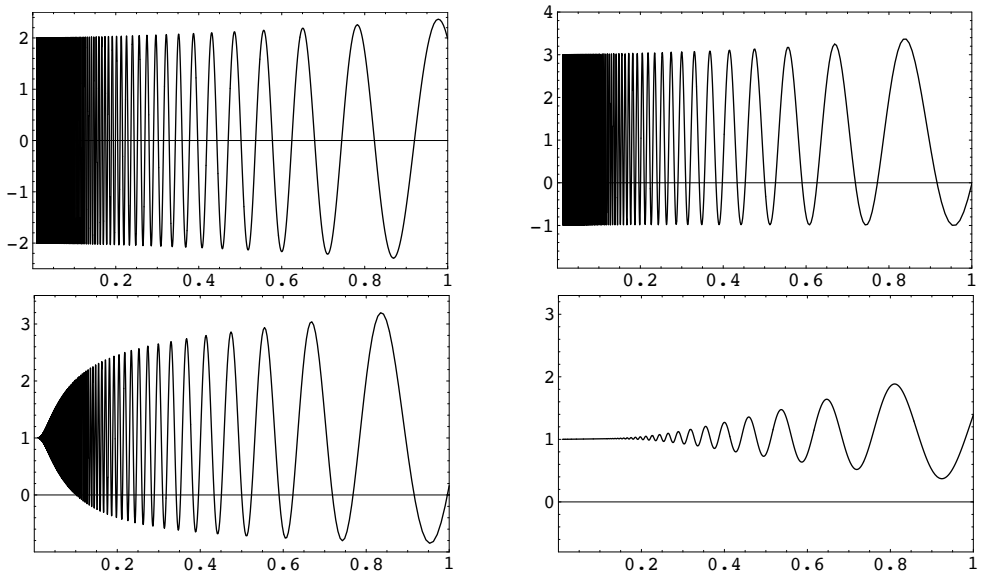

Figure 7: Quartic map with $r = \frac{3}{2}$: Transition from oscillating to monotone asymptotic behaviour of the normalised homoclinic invariant as φ crosses the critical line. All plots display $\hat{\omega}(h)/|\Theta(4)|$ against h. The value of ϕ increases from top to bottom and from left to right.

Oscillating asymptotic with $\phi = \varphi_{\rm cr}(r)$. Wee keep $r = \frac{3}{2}$ and compute $\varphi_{\rm cr}(r)$ numerically. We observe that the angle between W^u and W^s at the main homoclinic point oscillates as h decreases (see Figure 7 top right). Asymptotically $\hat{\omega}$ behaves like a sum of an oscillating (15) and non-oscillating (14) expansions:

$$\frac{\hat{\omega}(h)}{|\Theta(4)|} \asymp A_0(h) + A_1(h)\cos\left(\frac{2\pi\beta}{h} + \frac{2\pi}{3}\right) + B_1(h)\sin\left(\frac{2\pi\beta}{h} + \frac{2\pi}{3}\right),$$

where A_0, A_1, B_1 are formal series in powers of $h^{1/3}$ and $A_0(0) = 1$, $A_1(0) = 2$ and $B_1(0) = 0$.

We see that the behaviour of $\hat{\omega}$ is well described by the leading term of the asymptotic expansion. The situation is different if ϕ is close but not equal to $\varphi_{\rm cr}(r)$. If we fix r and increase ϕ to go through $\varphi_{\rm cr}(r)$, we see that the leading term of the asymptotic expansion has a jump from 1 to $2\cos\left(\frac{2\pi\beta}{h} + \frac{2\pi}{3}\right)$. On the other hand $\hat{\omega}$ is a smooth function of h, r and ϕ provided $h > 0$. A typical behaviour of $\hat{\omega}(h)$ near the transition is shown on Figure 7. On this picture we see, that if ϕ is slightly less than $\varphi_{\rm cr}(r)$, the homoclinic invariant oscillates for moderate h in a way similar to the critical case, but the oscillations decay first slowly and then virtually disappear near $h \approx 0.05$.

It is interesting to note that the oscillations behave like the sum of the contributions of the three complex singularities of x_0 with different heights over the real axis.

5 Singularities of separatrices

In this section we study separatrix solutions of the simple differential equation

$$\ddot{x}_0 = f(x_0), \tag{16}$$

subject to the condition

$$\lim_{t\to\pm\infty} x_0(t) = a_\pm.$$

The limits $a_\pm$ are roots of the function f: $f(a_+) = f(a_-) = 0$, and correspond to equilibria of the differential equation. We assume that $f'(a_\pm) > 0$, so the equilibria are hyperbolic saddle points. We will often discuss homoclinic solutions when $a_+ = a_-$.

Complex singularities of $x_0(t)$ play a crucial role in our study of the exponentially small separatrix splitting. In this section we discuss the problem of finding the singularities of x_0 from analytical and numerical viewpoints.

In some cases the separatrix solution can be found explicitly, their singularities can be found analytically, and their types can be easily determined.

In most cases there is no explicit solution for (16) in terms of elementary functions. Then the numerical integration can be useful.

It is interesting that assumptions on the type of the singularities of the separatrices can lead to very strong restrictions on the possible nonlinearities of f. For example, consider the following two statements:

- If f is an entire function and x_0 has a pole, then f is a polynomial of degree two or three.
- If f is an entire function and $\dot{x}_0$ has a simple pole, then f is a trigonometrical polynomial of degree one or two.

We conclude that if f is entire, $a_\pm$ are hyperbolic saddles and $\dot{x}_0$ has a pole, then the corresponding separatrix solution of the differential equation (16) is one of the described in the next subsection up to a substitution $x_0(t) \to ax_0(bt + c) + d$ for some $a, b, c, d \in \mathbb{R}$.

5.1 Explicit separatrix solutions

If f is polynomial of degree 2 or 3, we can describe all possible homoclinic and heteroclinic trajectories associated with hyperbolic equilibria of the differential equation (16). It is convenient to translate, scale and, if necessary, reflect the x-variable and to scale t in order to transform f to one of the following cases.

1. If f is polynomial of degree 2 and has two distinct real zeros, then it can be transformed to $x - x^2$ by mapping the zeroes to 0 and 1 respectively and scaling time.
2. If f is polynomial of degree 3 and the differential equation has a homoclinic or heteroclinic trajectory associated with hyperbolic saddles, then f necessarily has 3 distinct real roots. Depending on their positions and, in general, on coefficients of f, the following cases are possible:
   (a) The separatrices form a shape of "∞", which can be either symmetric or asymmetric.
   (b) There is a separatrix loop on one side of the hyperbolic saddle only, the other two separatrix "whiskers" go to infinity.
   (c) There is a heteroclinic trajectory connecting two hyperbolic saddles.

The corresponding reduced functions f, separatrix solutions and their singularities are given in Table 2. All the separatrix solutions have complex period $2\pi\mathrm{i}$ and are real-analytic. As a result it is sufficient to provide singularities in the strip $\Im t \in (0, \pi]$. Any other singular point can be obtained by reflection with respect to the real axis and translation by $2\pi\mathrm{i}k$, $k \in \mathbb{Z}$.

The last row of the table contains an example of a polynomial $f(x)$ of degree larger than 3. The corresponding separatrix is given explicitly. Its singularities are branching points and not poles.

Now we study the cases of trigonometrical polynomials of degree one and two. We always assume that the mean value of f over its period vanishes and we scale the least period of f to 2π.

If f is a trigonometrical polynomial of degree 1, it can be transformed to $f(x) = \sin x$. Then $x_0(t) = 4 \arctan \mathrm{e}^t$ with a logarithmic singularity at $\frac{\mathrm{i}\pi}{2}$.

n	$f(x)$	$x_0(t)$	Singularities	type
2	$x-x^2$	$\dfrac{3}{2\cosh^2(t/2)}$	$\mathrm{i}\pi$	pole of order 2
3 (a)	$x-x^3$	$\pm\dfrac{\sqrt{2}}{\cosh t}$	$\dfrac{\mathrm{i}\pi}{2}$	pole of order 1
3 (a')	$x+rx^2-x^3$	$\dfrac{3}{\sqrt{r^2+\frac{9}{2}}\cosh(t)-r}$	$\mathrm{i}\cot^{-1}\left(\dfrac{r\sqrt{2}}{3}\right)$	pole of order 1
3 (b)	$x-rx^2+x^3$	$\dfrac{3}{\sqrt{r^2-\frac{9}{2}}\cosh(t)+r}$	$\mathrm{i}\pi\pm\tanh^{-1}\frac{3}{\sqrt{2}r}$	poles of order 1
3 (c)	$-\dfrac{x}{2}+x^3$	$\dfrac{\tanh(t/2)}{\sqrt{2}}$	$\mathrm{i}\pi$	pole of order 1
$n\geq 4$	$x-x^n$	$\sqrt[n-1]{\dfrac{n+1}{2\cosh^2\frac{(n-1)t}{2}}}$	$\dfrac{\mathrm{i}\pi}{n-1}+\dfrac{2\pi\mathrm{i}k}{n-1}$	branching points

Table 2: Separatrix solutions of the differential equation $\ddot{x}_0 = f(x_0)$ and their singularities for different polynomial $f(x)$. The arccotangent is denoted by $\cot^{-1}$ and takes its values in the interval $(0,\pi)$. In the case 3 (a') $r\in\mathbb{R}$, and in the case 3 (b) $r>\frac{3}{\sqrt{2}}$.

If f is a trigonometric polynomial of degree 2, its most generic form depends on two amplitudes and two phases. On a period, it can have at most two simple zeros with positive derivatives. Assuming that at least one such zero exists, we translate it to the origin. Then scaling time we transform f to the form

$$f(x) = r_1\sin x + r_2\cos x + \frac{1-r_1}{2}\sin 2x - r_2\cos 2x\,.$$

In this way we have reduced the number of parameters to two, namely to r_1 and r_2.

If $r_1 > r_2^2$, the corresponding separatrix solution

$$x_0(t) = 2\pi - 2\mathrm{cot}^{-1}\left(r_2+\sqrt{r_1-r_2^2}\sinh t\right)$$

is monotonically increasing and connects $x=0$ and $x=2\pi$. It has logarithmic singularities at

$$t_* = \mathrm{arcsinh}\frac{\mathrm{i}-r_2}{\sqrt{r_1-r_2^2}}.$$

We should note that arcsinh is multivalued and the formula actually gives two singularities in the strip $\Im t\in(0,\pi]$, namely t_* and $\mathrm{i}\pi - t_*$. The imaginary parts of these singularities are equal if and only if $\Im t_* = \frac{\pi}{2}$. Using the explicit formula for t_* we conclude that this happens iff $r_2=0$ and $r_1\in(0,1)$.

If $r_1 < r_2^2$, then there are two solutions

$$x_0(t) = 2\mathrm{cot}^{-1}\left(-r_2\pm\sqrt{r_2^2-r_1}\cosh t\right)$$

bi-asymptotic to zero or 2π depending on the choice of the sign in the formula. The singularities are

$$t_* = \mathrm{arccosh}\frac{\mathrm{i}+r_2}{\pm\sqrt{r_2^2-r_1}},$$

respectively. The separatrix solutions are real-analytic and even. Consequently if t_* is a singularity then $t'_* = -\bar{t}_*$ also is. It has the same imaginary part and opposite real part. Since the real part does not vanish, $t_* \neq t'_*$. Therefore, x_0 has two different singularities on the line $\Im t = \rho$.

If $r_1 = r_2^2$, then there is a chain of two heteroclinic solutions, one of which connects 0 to the point $a_1 = 2\cot^{-1}(-r)$ and the second one connects a_1 to 2π. The solutions are given by

$$x_0(t) = 2\cot^{-1}(-r + \mathrm{e}^{-t}) \qquad \text{and} \qquad x_0(t) = 2\cot^{-1}(-r - \mathrm{e}^{t}),$$

respectively. Their singularities are respectively at $t_* = -\log(r + \mathrm{i})$ and $t_* = \mathrm{i}\pi + \log(r + \mathrm{i})$. Any other singular point can be obtained by reflection with respect to the real axis and translation by $2\pi\mathrm{i}k$, $k \in \mathbb{Z}$.

In these trigonometrical cases, x_0 has logarithmic singularities and all singularities of $\dot{x}_0$ are simple poles.

5.2 Singularities of implicitly defined separatrix solutions

In general a separatrix solution cannot be found explicitly in terms of elementary functions. Nevertheless a singularity of the separatrix can be represented explicitly in form of an integral. This fact is widely known, and the main goal of this section is to discuss appropriate choices for the integration path.

In this section we mainly consider the case of a polynomial $f(x)$ although many arguments and conclusions can be applied to non-polynomial functions. We also assume that the degree of f is larger than 3 as the problem have already been completely solved for lower degrees.

A zero a of f corresponds to an equilibrium. If $f'(a) > 0$ the equilibrium is a hyperbolic saddle. Without any loss in generality, we may assume that the saddle point is at the origin

$$f(0) = 0 \qquad \text{and} \qquad f'(0) = 1.$$

Let $F(x) = \int_0^x f(x)dx$. Then integrating equation (16) we obtain

$$\frac{\dot{x}_0^2(t)}{2} = F(x_0(t))$$

and

$$t = \int_{x_0(0)}^{x} \frac{ds}{\sqrt{2F(s)}}. \tag{17}$$

In order to find $x_0(t)$ it is necessary to invert the function $x \mapsto t$ defined by this integral. On the other hand the problem of finding singular points of x_0 does not require this operation. Indeed, let t_* be a singular point of x_0. Since $x_0(t)$ is unbounded at t_* we conclude

$$t_* = \int_{x_0(0)}^{\infty} \frac{dx}{\sqrt{2F(x)}}\,. \tag{18}$$

If convergent, the integral represents a singularity of x_0. The integral is taken along a path which avoids zeroes of F on the complex plain. The value of the integral depends on the homotopy class of the path. It is not difficult to construct a polynomial, such that the set of all possible values of the integral are dense in $\mathbb{C}$.

On the other hand it is not difficult to prove that there is $\rho > 0$ such that x_0 is analytic in a strip $|\Im t| < \rho$ and has a finite number of singularities on its boundary.

This does not contradicts to the density of singularities, since x_0 is multivalued and other singular points mostly belong to different sheets of the Riemann surface of x_0.

We are interested in finding the singularities on the first sheet of the Riemann surfaces, which requires a procedure for identification of suitable paths.

We say that a singular point $t_* \in \mathbb{C}$ is *visible* (*from the real axis*), if x_0 can be continued from the real axis along the vertical line $\gamma(s) = \Re t_* + s\mathrm{i}$ for $s \in (0, \Im t_*)$ but not to $s = \Im t_*$. Note that γ connects the points $\Re t_*$ and t_*.

As x_0 is real analytic, if t_* is a visible singularity, then $\bar{t}_*$ is also visible. Therefore visible singularities come in pairs. The separatrix solutions of the differential equation are never entire and, therefore, every separatrix solution has at least two visible singularities.

If f is polynomial there is an easy upper bound on the number of visible singularities.

Lemma 1 *If f is a real polynomial of degree $n \geq 2$ and x_0 is a separatrix solution of equation* (16)*, then the number of visible singularities is never larger than $2n-2$.*

Moreover, if additionally the separatrix forms a figure "∞", then the total number of visible singularities for the left and right separatrix branches together is not larger than $2n-2$. In particular, the number of visible singularities for one of the "whiskers" is not larger than $2n-4$.

Proof. We sketch the proof of the lemma. Consider the equation

$$X'' = -f(X) \quad \text{subject to the initial conditions } X(0) = x,\ X'(0) = \mathrm{i}\sqrt{2F(x)}. \tag{19}$$

We assume that $x \in \mathbb{C}$ and the "time" $s \geq 0$. In the essence, we study the differential equation

$$(X'(s))^2 = -2F(X(s)),$$

which describes the evolution of a point $(X(s), X'(s))$ moving on the Riemann surface $Y^2 = -2F(X)$. The form (19) is more convenient for numerical experiments, because it allows us to choose a branch of the square root at the initial point only.

Since $(X'(s))^2 = -2F(X(s))$ for all s and all initial conditions x, different semi-trajectories do not intersect each other. There are no self-intersections except for the case when $X(s)$ goes through a return point, i.e. $F(X(s_0)) = 0$ with $F'(X(s_0)) \neq 0$ for some s_0. In this case, $X'(s_0) = 0$ and the trajectory is symmetric with respect to s_0: $X(s_0 + s) = X(s_0 - s)$ due to the time-reversible symmetry of the equation.

Using the fact that the polynomial f behaves like x^n for $|x| \gg 1$, it can be shown that the number of different unbounded positive semi-trajectories is exactly $n-1$.

There is a simple relation between unbounded semi-trajectories and visible singularities. If t_* is a visible singularity, then the initial condition $X(0) = x_0(\Re t_*)$ leads to an unbounded positive semi-trajectory for one of two possible choices of the branch of the square root.

Let $M = \sup_{t\in\mathbb{R}} x_0(t)$, which coincides with the smallest positive zero of F. If $x \in (0, M]$ corresponds to an unbounded semi-trajectory, then there is a corresponding visible singularity.

If the path in the integral (18) is homotopic to the union of two curves: the first one connects $x_0(0)$ and $X_0(0)$ along the real axis and the second one is the unbounded semi-trajectory $X_0(s)$, then the value of the integral coincides with the visible singularity t_*.

The second part of the lemma follows from the observation that both branches of the separatrix belong to the same Riemann surface and that a semi-trajectory which intersects the real axis twice is necessarily periodic due to the real analytic symmetry. Therefore an unbounded semi-trajectory intersect at most one of the separatrix "whiskers", and we get an upper bound for the total number of visible singularities. □

Remark 2 *If $f(x) \to -\infty$ for $x \to +\infty$, then an unbounded semi-trajectory, when it approaches the infinity, follows one of the asymptotic directions defined by $\arg x = \frac{2\pi k}{n-1}$, $k \in \{0, 1, \ldots, n-2\}$.*

If $f(x) \to +\infty$ for $x \to +\infty$, then the directions are rotated by the angle $\frac{\pi}{n-1}$.

Remark 3 *In the examples presented in this paper all solutions of the equation* (19) *are either periodic or unbounded. Periodic trajectories form continuous families and inside each one the period is constant. The unbounded trajectories act as separatrices between families of periodic ones.*

In particular, every trajectory sufficiently close to the origin is periodic with period 2π due to the normalisation $f'(0) = 1$.

This is a typical situation, but in principle different types of behaviour are possible. For example, if the function F has a complex multiple zero b such that $F(b) = F'(b) = 0$ and $\Im F''(b) \neq 0$, then a semi-trajectory may converge to this point.

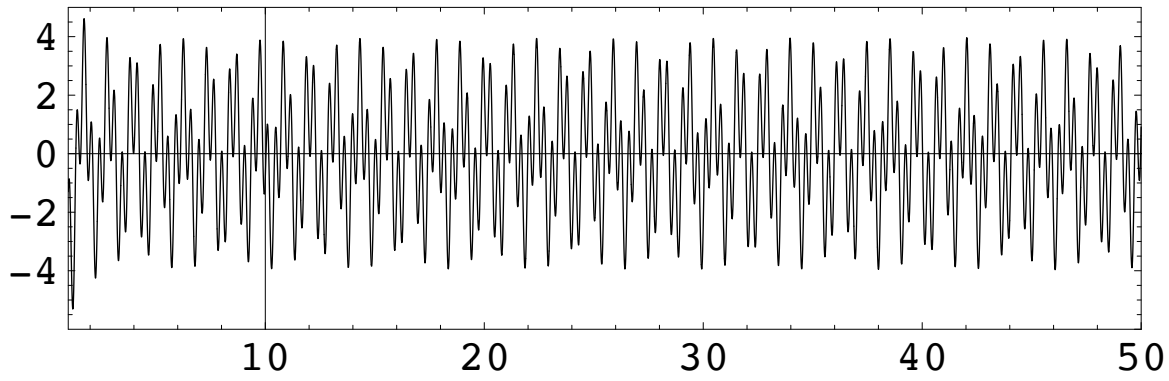

Figure 8: Normalised homoclinic invariant for a polynomial of degree 6 plotted as a function of h^{-1}.

If the nonlinearity f in equation (16) is polynomial of degree n, every separatrix associated with hyperbolic fixed points has m, $1 \le m \le n-1$, pairs of visible singularities at t_j and $\bar{t}_j$, $1 \le j \le m$. Moreover, there are curves Γ_j, $1 \le j \le m$, with the following properties:

- $t_j = \displaystyle\int_{\Gamma_j} \frac{dx}{\sqrt{2F(x)}}$ is a visible singularity of x_0, $0 < \Im t_j \le \pi/\sqrt{f'(0)}$.
- $\Gamma_j(0) = x_0(0)$
- $\lim\limits_{s\to\infty} |\Gamma_j(s)| = \infty$ and $\lim\limits_{s\to\infty} \arg\Gamma_j(s) = \dfrac{2\pi k_j}{n-1}$, where $0 \le k_j \le n-2$ is an integer.
- $k_{j_1} \ne k_{j_2}$ if $j_1 \ne j_2$.
- There are neither pairwise intersections nor self-intersections.
- There are no other visible singularities of x_0.

In actual computations we evaluated the integral (18) along straight lines from $x_0(0)$ to infinity adjusting their directions to find a line in the homotopy class of Γ_j. In principle, the homotopy class of Γ_j does not necessarily contain a straight line. In this situation, a more accurate computation of the unbounded semi-trajectories defined earlier in this section may be necessary to determine the homotopy class of Γ_j.

A good indication about the number of visible singularities can be obtained from a plot of trajectories of the points $x = z_j$, where $F(z_j) = 0$.

Remark 4 *The absolute value of the imaginary part of the leading visible singularity is not larger than* $\frac{\pi}{\sqrt{f'(0)}}$. *It follows from the fact that* x_0 *is analytic and periodic with period* $\frac{2\pi\mathrm{i}}{\sqrt{f'(0)}}$ *in the complex half-plane* $\Re t < \Re t_*$.

5.3 Conclusions. Other phenomena

In the case of a polynomial of degree 6, we adjusted coefficients of the function f in such a way that the separatrix of the differential equation (7) has 4 leading singularities with equal imaginary part. As expected the normalised homoclinic invariant oscillated similar to a quasi-periodic function of h^{-1} (see Figure 8). We note that it is not actually a quasiperiodic function but converges to a sum of two sinusoidal functions of equal amplitude as h goes to 0. This phenomenon has co-dimension 1.

We also found a polynomial of degree 5, which has separatrices with the shape of a figure "eight", such that the right hand side has an oscillating asymptotic and the left hand side is monotone as a function of h.

If f is a rational function, then the leading singularity of the unperturbed separatrix can be of two different kinds: unbounded at the singular point or related to a pole of f. In the former case, the asymptotic behaviour of ω was observed to be similar to the polynomial case with a splitting constant $\Theta(n)$. In the latter case, the behaviour depends on the order of the pole. If the order is larger than 2, the asymptotic formulae of Section 2 seem to be valid if n equals minus the order of the pole. The sequences of constants $|\Theta(n)|$ has to be extended to negative n. The case $n = -1$ is special and even the leading term of the asymptotic is not known.

Acknowledgements

This work is partially supported by the EPSRC grant EP/C000595/1. The first author also thanks the Nuffield Foundation for the support during the early stages of this work. The second author has been supported by grants BFM2003-09504-C02-01, MTM2006-05849/Consolider(Spain) and CIRIT 2005 SGR-1028 (Catalonia).

References

[1] Delshams, A., Ramírez-Ros, R., Melnikov potential for exact symplectic maps. Comm. Math. Phys. 190 (1997), no. 1, 213–245.

[2] Delshams, A., Ramírez-Ros, R., Singular separatrix splitting and the Melnikov method: an experimental study. Experiment. Math. 8 (1999), no. 1, 29–48.

[3] Fontich, E.; Simó, C., The splitting of separatrices for analytic diffeomorphisms. Ergodic Theory Dynam. Systems 10 (1990), no. 2, 295–318.

[4] Gelfreich, V., Lazutkin, V., Tabanov, M., Exponentially small splittings in Hamiltonian systems. Chaos 1 (1991), no. 2, 137–142.

[5] Gelfreich, V. G. A proof of the exponentially small transversality of the separatrices for the standard map. Comm. Math. Phys. 201 (1999), no. 1, 155–216.

[6] Gelfreich, V., Lazutkin, V., Splitting of separatrices: perturbation theory and exponential smallness. Russian Math. Surveys 56 (2001), no. 3, 499–558.

[7] Lazutkin, V. F., Splitting of separatrices for the Chirikov standard map, J. Math. Sci. 128 (2005), no. 2, 2687–2705 (translated from the Russian manuscript originally published in VINITI 1984).

[8] Sanders, J., Melnikov's method and averaging. Celestial Mech. 28 (1982), no. 1-2, 171–181

[9] Simó, C., Analytical and numerical detection of exponentially small phenomena. Equadiff 1999, Vol. 1, 2 (Berlin, 1999), 967–976, World Sci. Publ.

[10] Simó, C., Vieiro, A., Some relevant aspects of area preserving maps and the planar conservative Hénon map. Preprint (2006), Univ. Barcelona.